J Food Sci Technol (April 2021) 58(4):1511–1523
https://doi.org/10.1007/s13197-020-04664-3

ORIGINAL ARTICLE

Effects of simulated digestion on black chokeberry (*Aronia melanocarpa* (Michx.) Elliot) anthocyanins and intestinal flora

Wenchen Yu[1] · Jun Gao[2] · Ruobing Hao[1] · Jing Yang[1] · Jie Wei[1]

Revised: 5 June 2020 / Accepted: 31 July 2020 / Published online: 11 August 2020

Abstract In this study, the changes of anthocyanin content, total phenols, antioxidant capacity, microbiota composition before and after digestion and intestine fermentation in stomach and intestine were studied. The results indicated that after simulated gastrointestinal digestion, compared with the original sample, the total phenol content and anthocyanin content of intestinal digestion group for 2 h (ID 2 group) decreased by 53.64% and 70.45%, respectively, DPPH inhibition rate was 32.75% and T-AOC values of the extracts decreased to 62.89U/mg. The anthocyanins were identified to be composed of cyanidin-3-arabinoside, cyanidin-3-galactoside, cyanidin-3-xyloside, and cyanidin-3-glucoside. Black Chokeberry (*Aronia melanocarpa* (Michx.) Elliot) anthocyanins significantly increased the relative richness of *Bacteroides*, promoted the growth of *Bifidobacterium*, *Blautia*, *Faecalibacterium*, and inhibited the growth of *Prevotella*, *Megamonas*, *Escherichia/Shigella*, etc. Anthocyanins have a positive regulatory effect on intestinal flora. These studies also provide essential information for the development of anthocyanin related health care products and drug products.

Keywords Anthocyanins · Antioxidant capacity · Biotransformation · Intestinal microflora

Wenchen Yu and Jun Gao two authors should be regarded as joint first authors.

✉ Jie Wei
J.Wei2015@hotmail.com

[1] School of Life Science, Liaoning University, Chongshan Middle road 66, Huanggu District, Shenyang 110036, Liaoning, China

[2] Liaoning Forestry Academy, Shenyang 110032, China

Introduction

Less known fruits are genetically very diverse groups grown in different parts of the world and have been recognized for their human health benefits. Most of the less known fruits attracted peoples due to high content of non-nutritive, nutritive, and bioactive compounds such as flavonoids, phenolics, anthocyanins, phenolic acids, and as well as nutritive compounds such as sugars, essential oils, carotenoids, vitamins, and minerals (Fazenda et al. 2019; Halasz 2010; Senica and Mikulic 2019) Black Chokeberry (*Aronia melanocarpa* (Michx.) Elliot) is a perennial deciduous shrub of the family *Rosaceae*, Black Chokeberry (*Aronia melanocarpa* (Michx.) Elliot) fruit contains rich nutrients such as dietary fiber, sugar, protein, and polyphenolic compounds (Kulling and Rawel 2008; Tanaka 2001). The polyphenols in the fruit mainly include phenolic acids, proanthocyanidins, anthocyanins, flavonols, etc. The anthocyanin content is as high as 1%, accounting for about 25% of total phenols (Appel et al. 2015). In terms of oxygen free radical scavenging capacity (ORAC), the Black Chokeberry (*Aronia melanocarpa* (Michx.) Elliot) has the highest antioxidant activity than other fruits. However, due to the poor taste of the fruit itself, it is particularly important to take a suitable food extraction and preservation process. At present, the more advanced non-thermal technologies include the use of ultrasound and antimicrobial agents, etc., which can effectively maintain the sensory and nutritional characteristics of fresh food (Daniel et al. 2018; Galanakis 2015; Zinoviadou et al. 2015).

Anthocyanins has anti oxidation, anti-cancer, anti-inflammation, prevention of urinary tract infection, treatment of diabetes, protect liver and treat obesity. Its extract has a significant effect on the prevention and treatment of

cardiovascular and cerebrovascular diseases. It has been reported that dietary polyphenols can promote the growth of probiotic *Lactobacilli* and inhibit harmful bacteria *Staphylococcus*, *Salmonella* (Nohynek et al. 2005). It is generally believed that dietary polyphenols, especially anthocyanins, have the ability to regulate intestinal microflora (Jamar et al. 2017). Therefore, in order to realize the health promoting properties of anthocyanins, the interaction between anthocyanins and intestinal microflora must be considered to understand their biological functions.

Intestinal tract is not only the digestion place of human body, but also the largest immune organ of human body (Park et al. 2017). It is rich in a large and complex microbial community. It has been reported that the human microbiota is mainly composed of *Firmicutes*, *Bacteroidetes*, *Proteobacteria*, *Actinobacteria*, *Fusobacteria* and *Verrucomicrobia* (Gill et al. 2006). There are more than 800 species and 7000 strains of bacteria, showing great diversity at the subspecies or strains level. 97–99% of human intestinal flora is anaerobes, and the structure of intestinal flora is relatively stable (Yuki et al. 2018). Intestinal flora plays an important role in energy intake, absorption and storage, production of important metabolites, moistening intestinal epithelial cells, participating in inflammatory response and regulating immune function (Rivière 1997). There is a close correlation between human intestinal flora and the occurrence and development of diabetes, obesity and other metabolic diseases (Jung et al. 2015). It is pointed out that polyphenols can stimulate the production of short chain organic acids in intestinal flora, and the fermented polyphenols can promote the proliferation of *Bifidobacteria*, reduce the number of intestinal *Enterobacteria*, improve the healthy growth of the body, and affect the composition and diversity of intestinal mucosal microorganisms (Turroni et al. 2017). However, the bioactive substances ingested by the body will be degraded or transformed in the process of gastrointestinal digestion, so the ingested bioactive substances cannot be fully utilized by the body. Therefore, bioavailability is one of the main factors affecting the efficacy of bioactive substances on human body. Using the method of simulated digestion in vitro to study the biological activity of substances is closer to the situation that substances are used by organisms. It has reported that the stability and metabolites of anthocyanin in *Lycium ruthenicum Murray* extract have been studied by simulating gastrointestinal digestion in vitro (Ryu and Koh 2018). The in vitro digestion simulation technology has the advantages of simplicity, rapidity, low cost and good reproducibility. The establishment of this technology is of great significance to accurately evaluate the biological activity of substances (Rosacmillán et al. 2020). At present, there are few studies on the stability of external digestion of Black Chokeberry (*Aronia melanocarpa* (Michx.) Elliot). In this study, the effects of total phenol, total anthocyanin content, anthocyanin composition and intestinal microflora on anthocyanin of Black Chokeberry (*Aronia melanocarpa* (Michx.) Elliot) before and after gastrointestinal digestion and colon fermentation were studied. With the promotion of planting and the deepening of people's understanding of its health care function, the research on the deep processing of fruit will be further deepened and improved. Nowadays, polyphenols are widely used in food additives (Galanakis 2018), cosmetics manufacturing and other industries (Galanakis et al. 2018). It is believed that the products of the fruit processing of Black Chokeberry (*Aronia melanocarpa* (Michx.) Elliot) will be paid more and more attention by consumers and get the attention of the health care industry, in order to provide reference for the food research and health care product development of Black Chokeberry (*Aronia melanocarpa* (Michx.) Elliot).

Materials and methods

Chemicals and materials

Gallic acid, protocatechuic acid, DPPH (1,1-diphenyl-2-picrylhydrazyl) were purchased from Tiangen Biotech Co., Ltd. (Beijing, China). T-AOC (A105) was purchased from Jiangcheng, Nanjing Bioengineering Co., Ltd. (Nanjing,China). Pepsin and pancreatin were purchased from Sangon Biotech Co., Ltd. (Shanghai, China). Black Chokeberry (*Aronia melanocarpa* (Michx.) Elliot) was provided by Liaoning Academy of Forestry (Shenyang, China).

Extraction of anthocyanins

The procedures for extraction of anthocyanins were performed according to Swer et al. (2018), with some modifications. Briefly, Black Chokeberry (*Aronia melanocarpa* (Michx.) Elliot) fruit were extracted by impregnating with MeOH (0.5% trifluoroacetic acid, TFA V/V) at room temperature for 24 h and evaporating most of the solvent in vacuum. Ultrasonic extraction at 37 °C for 30 min, followed by vacuum filtration. Ethyl acetate (4 × 0.5 L) separated the condensed extract (0.5 L) and discarded the organic phase. The filtrate was filled with AB-8 macroporous resin. After 24 h of oscillating adsorption in a constant temperature oscillator, impurities were removed by deionized water, 60% ethanol acidified by 0.1% HCl was used as eluent. The eluent was rotated repeatedly to evaporate, and the eluent was removed. The concentrated

liquid was separated into 10 mL centrifugal tubes and stored in − 20 °C refrigerator for reserve.

Simulated gastric digestion

The procedures for simulated gastric digestion were carried out according to Chen et al. (2019), with some modifications. Gastric digestion: Dissolve 200 mg Black Chokeberry (*Aronia melanocarpa* (Michx.) Elliot) anthocyanins (AMA) in 50 mL 0.9% NaCl solution, add appropriate 1 mol/L HCl solution to adjust pH to 2, add 160 mg pepsin (3000 U/mg pro). The mixture was immediately sealed with nitrogen and placed in a constant temperature shaking incubator at 37 °C for 2 h. Repeat the experiment three times.

Simulated small intestine digestion

The procedures for simulated intestinal digestion were carried out according to Wang et al. (2019), with some modifications. Intestinal digestion: 0.5 mol/$NaHCO_3$ solution was added dropwise to the above simulated gastric juice and neutralized to pH 6, and then 18 mL-cholate buffer (2 mg/mL pancreatin (250 U/mg pro), 12 mL/mL cholate, V/V = 12:6), then adjust the pH to 7.5 with 0.5 mol/$NaHCO_3$ solution. The mixture was immediately sealed with nitrogen and placed in a 37 °C constant temperature shaking incubator for 2 h. After sampling, acidify with phosphoric acid (V/V = 17:3) to pH = 2, centrifugate at 12,000 × g and 4 °C for 10 min, take the supernatant and store it at 4 °C for later use. Repeat the experiment three times.

Co-culture of human fecal microorganisms and anthocyanins

The procedures for simulated fermentation were carried out according to Chena et al. (2017), with some modifications. Firstly, the fresh feces for experiments were collected from 5 healthy volunteers (3 men and 2 women, 22–28 years old) not taken antibiotics at least three months, volunteers are healthy and eat normally. 50 mL (100 mm, pH = 7.3) potassium phosphate buffer was added into the sterile environment, and store in the refrigerator for standby. Composition of nutrient growth medium: peptone 3.0 g/L, yeast extract 3.0 g/L, hemim 0.02 g/L, cysteamine hydrochloride 0.8 g/L, bile salts 0.5 g/L, hemoglobin 0.05 g/L, Tween 80 2.0 mL/L, vitamin K1 10 μL/L (Sangon, Shanghai, China). Trace element composition: 0.24 g $NaS{\cdot}7H_2O$, 3.30 g $CaCl_2{\cdot}2H_2O$, 2.50 g $MnCl_4{\cdot}H_2O$, 0.25 g $CoCl_2{\cdot}6H_2O$ and 2.00 g $FeCl_3{\cdot}6H_2O$ (Sangon, Shanghai, China) were weighed respectively. Dissolve the above four compounds with 250 ml deionized water, add 300μL microelement buffer every 1 ml nutrient growth media. The mixture of anthocyanin (1 g/L), fecal slurry suspension 1 mL and growth nutrition medium 9 mL was recorded as AMA group; tea polyphenol (1.0 g/L) fecal slurry suspension 1 mL and growth nutrition medium 9 mL was recorded as EGCG group, basic nutrient culture without carbon source as blank control, recorded as BLK group. The flora of human fecal suspension was recorded as CON group. In the anaerobic incubator, fill each tube with nitrogen, immediately plug the plug with a rubber stopper, conduct anaerobic culture for 5 h, and repeat the experiment three times.

Determination of total phenolic content

Accurately measure 1 mL of Folin-phenol reagent in the test tube, add 200 μL of sample solution with appropriate dilution, after 4 min of room temperature reaction in dark, add 800 μL of Na_2CO_3 solution (75 g/L), and keep the balance in dark for 2 h. Absorbance measurement of reaction mixture at 765 nm wavelength. Undigested group was recorded as UD; Stomach digestion 1 h was recorded as SD 1; Stomach digestion 2 h was recorded as SD 2; Intestinal digestion 1 h was recorded as ID 1; Intestinal digestion 2 h was recorded as ID 2. The regression equation was $y = 0.08105 + 5.01143x$ ($R^2 = 0.9996$). Results expressed in mg GAE/L of sample solution with the equivalent of mg GAE/L (Şahin et al. 2018). Experiment repeated 3 times and averaged.

Determination of anthocyanin content

The content of total anthocyanins was determined by the reported method (Alara et al. 2017). The absorbance of the samples was measured at 520 and 700 nm at pH 1.0 and 4.5, respectively. The anthocyanin content was measured in terms of cyanidin-3-glucoside equivalent. The experiment was repeated 3 times and averaged.

$$\text{Anthocyanin content}(\text{mg/g}) = \frac{A \times MW \times DF \times DV \times 1000}{\varepsilon \times L}$$

where $A = (A_{520\ nm} - A_{700\ nm})_{pH\ 1.0} - (A_{520\ nm} - A_{700\ nm})_{pH\ 4.5}$, MW is the molecular weight of cyanidin-3-glucoside (449.2 g/mol), DF is dilution factor, DV is the total volume (mL), ε is the extinction coefficient for cyanidin 3-glucoside (26,900 L/mol/cm), W is the sample weight (g), and L is path length (1 cm). 10^3 is convert from g to mg.

T-AOC value determination

Using T-AOC kit (Jiangcheng, Nanjing, China) to detect the change of T-AOC value of anthocyanin. The groups

were same as described in 2.6. Calculate according to the formula. The experiment was repeated 3 times and averaged.

$$\mathrm{T-AOC\ (U/mg)} = \frac{\Delta \mathrm{OD} \times \mathrm{Total\ volume\ of\ reaction\ solution/mL}}{0.01 \times 30 \times \mathrm{Sampling\ /mL} \times \mathrm{Liquid\ concentration/(mol/L)}}$$

where ΔOD = OD of Determination − OD of Control.

DPPH inhibition determination

The groups were same as described in 2.6. The procedures for DPPH inhibition determination were carried out according to Suzihaque et al. (2017), with some modifications. 0.2 mmol/l DPPH · ethanol solution was prepared from anhydrous ethanol and stored at 4 °C. Add 2 mL of the test sample solution and 2 mL of DPPH solution to the same tube, and leave it in the dark for 30 min at room temperature, and then determine its absorbance at 517 nm as Ar. The absorbance of 2 mL of DPPH solution mixed with 2 mL of solvent (distilled water or corresponding buffer solution) as Ao, and the absorbance of 2 mL of the test sample solution mixed with 2 mL of absolute ethanol as As. DPPH inhibition is calculated according to equation. The experiment was repeated 3 times and averaged.

$$\mathrm{Y} = \left[1 - \frac{\mathrm{As} - \mathrm{Ar}}{\mathrm{Ao}}\right] \times 100\%$$

HPLC–MS/MS analysis

Anthocyanins were identified using Waters® 1288 ultra-performance liquid chromatograph system (Agilent Technologies, Waldbronn, Germany). The UPLC system was coupled with a quadruple-time-of-flight-tandem mass spectrometry (Q-TOF-MS/MS) system (SYNAPTTM G2) equipped with electrospray ionization (ESI). The samples in different treatment stages were dissolved in an appropriate amount of methanol, and the analytical chromatographic conditions were as follows. Column: AQ-C18 250 × 4.6 mm, 5um, temperature 25 degrees Celsius, injection volume 20 μL, photodiode array detector, detection wavelength 520 nm; injection volume: 20 μL; mobile phase: 0.05% trifluoroacetic acid water: acetonitrile; flow rate 0.7 mL/min; Gradient elution procedure, mobile phase: A: 0.05% trifluoroacetic acid water; B: acetonitrile 0–45 min A: 100–55%; 45–47 min A: 55–100%, 47–52 min A: 100%.

Mass spectrometry condition: Positive ion mode, fully automatic two-stage mass spectrometry scanning, scanning range: 50–1000 m/z; dry gas pressure: 2.76 × 105 Pa; flow rate: 12 L/min; temperature: 350 °C, capillary voltage: 3500 V.

Identification of intestinal microbiota (16sDNA sequencing)

After fermentation, the DNA of total bacteria was extracted with Stool DNA Kit (Sangon, Shanghai, China) for 16S rDNA sequencing. Under − 20 °C preservation and dry ice conditions, the DNA samples were sent to Center for Genomic Analysis Sangon Biotech (Shanghai) Co., Ltd. (Shanghai, China). High fidelity polymerase chain reaction (PCR) was used to amplify the V3 region of bacterial 16S rDNA with primers. The primer sequences were as follows: 341F (5′-ATTACCGCGGCTGCTGG-3′), 534R (5′-CGCCCGCCGCGCGCGGCGGGCGGGGCGGGGGCA-CGGGGGGCCT ACGGGAGGCAGCAG-3′). Length threshold 200 bp. PCR conditions: 94 °C denaturation for 4 min; 94 °C denaturation for 1 min, 65 °C annealing for 1 min, 72 °C extension for 4 min; 20 cycles; 94 °C denaturation for 1 min, 55 °C annealing for 1 min, 72 °C extension for 1 min, 5 cycles; 72 °C extension for 10 min. In the second round of amplification, Illumina bridge PCR compatible primers were introduced for high-throughput sequencing. All the results were based on sequenced reads and operational taxonomic units (OTUs).

Statistical analysis

SPSS 16.0 software was used for statistical analysis. All experiments were performed in at least tri-plicate for three separate biological repeats. One-way analysis of variance (ANOVA) followed by Dunnett's test was performed to compare more than two groups. Data are presented as the mean ± SD, and the significance level was set at $p \leq 0.05$.

Results and discussion

Simulated gastrointestinal digestion on the content of total polyphenols and total anthocyanins

There was no significant difference in total phenol and anthocyanins content after simulated gastric digestion (Fig. 1). Only a small part of anthocyanins was utilized by the stomach, and most of anthocyanins are utilized by the small intestine or metabolized by the intestinal microflora, resulting in the low bioavailability of anthocyanins. Anthocyanin was stable in at lower pH values (pH < 2.0) (Lee et al. 2015). The total anthocyanins contents of purple rice reduced by 76% after intestinal digestion (Sun et al.2015). There was no significant change in the total anthocyanin content of blueberry after gastric digestion

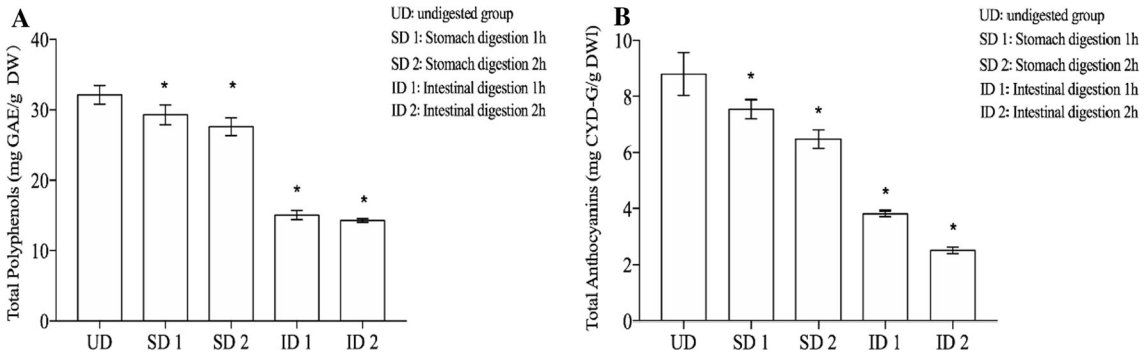

Fig. 1 Contents of anthocyanins in samples of UD group, SD 1 group, SD 2 group, ID 2 group, ID 2. **a** Total polyphenol; **b** total anthocyanin (mg/L). Values are means of three experiments performed in triplicate (three independent measures), with standard deviations depicted by vertical bars. Mean values were significantly different from those of the control group: $*p < 0.05$

(Correa et al. 2014). The results showed that the dissociation degree of anthocyanin increased with the increase of pH value (Nilufer-Erdil 2014). The higher the pH value, the higher the dissociation degree of anthocyanin. At present, the widely anthocyanins used extraction methods are solvent extraction (Ryu and Koh 2018), pressurized extraction (Bursać Kovačević et al. 2018), enzyme extraction, etc. (Zhang et al. 2020). Lycopene and pectin can be quickly and efficiently extracted from pink guava puree by centrifugation and separation with water-induced complexation (Nagarajan et al. 2019); Using "green" pressurized hot water extraction (PHWE) to extract the active substances from Stevia rebaudiana Bertoni leaves can increase the content of steviol glycosides and total phenols (Bursać Kovačević et al. 2018). The extraction of anthocyanins by ultrasound-assisted method was used in our experiment. Next, the anthocyanins were studied by simulated digestion experiment in vitro. At the end of simulated gastric digestion, the content of total phenol and total anthocyanin decreased. According to the original concentration, the contents of total polyphenols after simulated gastric digestion 1 h and 2 h were 29.3 ± 1.9 mg/g, 27.52 ± 1.79 mg/g, lost 9.32% and 14.42%, the contents of total anthocyanins were 7.56 ± 0.48 mg/g, 6.49 ± 0.57 mg/g, lost 11.3% and 24.26% respectively. After 1 and 2 h of simulated intestinal digestion, the contents of total polyphenols were 15.06 ± 0.93 mg/g, 14.29 ± 0.37 mg/g, lost 50.22% and 53.64% respectively, the total anthocyanin content were 3.84 ± 0.15 mg/g, 2.52 ± 0.16 mg/g, lost 54.39% and 70.45% respectively.

Identification and quantification of anthocyanins

The results of HPLC-MS/MS identification of anthocyanin showed that there were four absorption peaks in the HPLC spectrum of AMA at 520 nm (Fig. 2a). The elution order of peaks 1–4 was identical to that in earlier studies (Worsztynowicz et al. 2014). The retention time of peak 1 was 24.87, molecular ion peak was 449 (m/z), and ion fragment peak was 287 (m/z). The retention time of peak 2 is 25.71, molecular ion peak is 449 (m/z), and ion fragment peak is 287 (m/z). By referring to the identification literature of anthocyanin species, we can see that the monomer of anthocyanin aglycone m/z 287 is cyanidin, and further infer that the first peak is cyanidin-3-galactoside, and the second peak is cyanidin-3-glucoside. The retention time of the third peak is 26.88, the molecular ion peak is 419 (m/z), the ion fragment peak is 287 (m/z). The retention time of the third peak is 29.18, the molecular ion peak is 419 (m/z), the ion fragment peak is 287 (m/z). The cyanidin glycoside molecule loses a pentasaccharide aglycone structure. According to the references of anthocyanin species identification, it was deduced that the peak 3 was cyanidin-3-arabinoside and the peak 4 was cyanidin-3-xylose (Table 1). The molecular structure of the four anthocyanins is shown in the Fig. 2f. After simulated gastrointestinal digestion in vitro, the composition of four anthocyanins also changed (Fig. 2). It shows that the digestion affects the composition of anthocyanin, this is the same trend as the content change of blueberries anthocyanin after gastrointestinal digestion (Ji 2014). After digestion, the content of cyanidin-3-galactoside was the highest (Table 2). After fecal fermentation, cyanidin-3-xylose and cyanidin-3-glucoside were not detected. Anthocyanins were degraded in the intestinal digestion stage, so that they can be absorbed and utilized (Colin 2006). Therefore, this study explored the effect of anthocyanin on intestinal flora.

Digestion of anthocyanins in gastric and small intestine fluids and fermentation in vitro

The HPLC profile of anthocyanin degradation products at 254 nm is as shown in the Fig. 2e, the signal peak of protocatechuic acid standard was the same as that of AMA fecal fermentation broth at about 19 min. It is suggested that protocatechuic acid is one of the degradation products

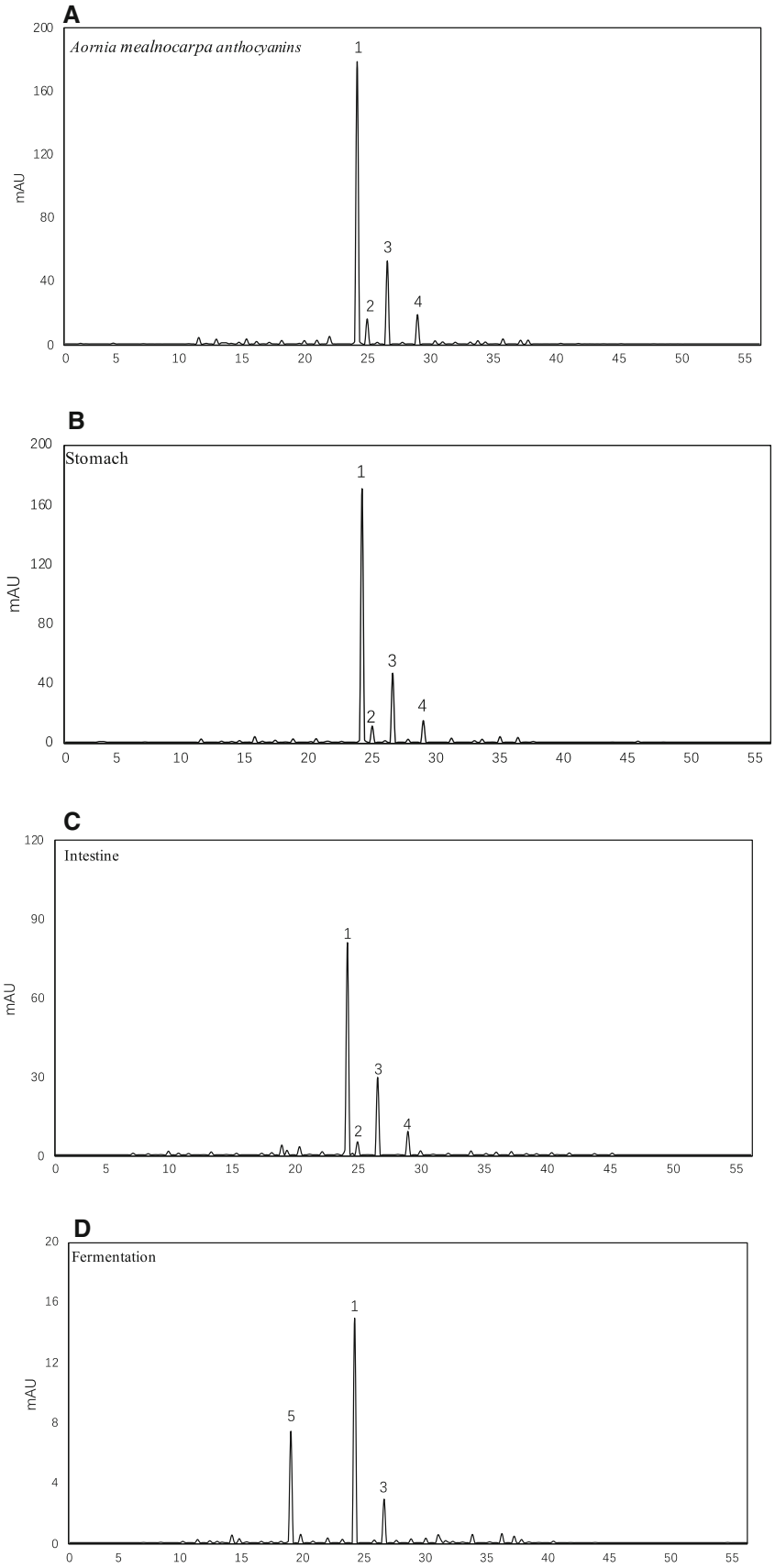

Fig. 2 High-performance liquid chromatograph profiles of *Aronia melanocarpa* extracts extract and in vitro gastrointestinal digestion **a** *Aronia melanocarpa* anthocyanin; **b** Stomach; **c** intestinal; **d** Fermentation; **e** Protocatechuic acid; **f** Molecular structure of cyanidin 3-galactoside, cyanidin 3-glucoside, cyanidin 3-arabinoside and cyanidin 3-xyloside

Fig. 2 continued

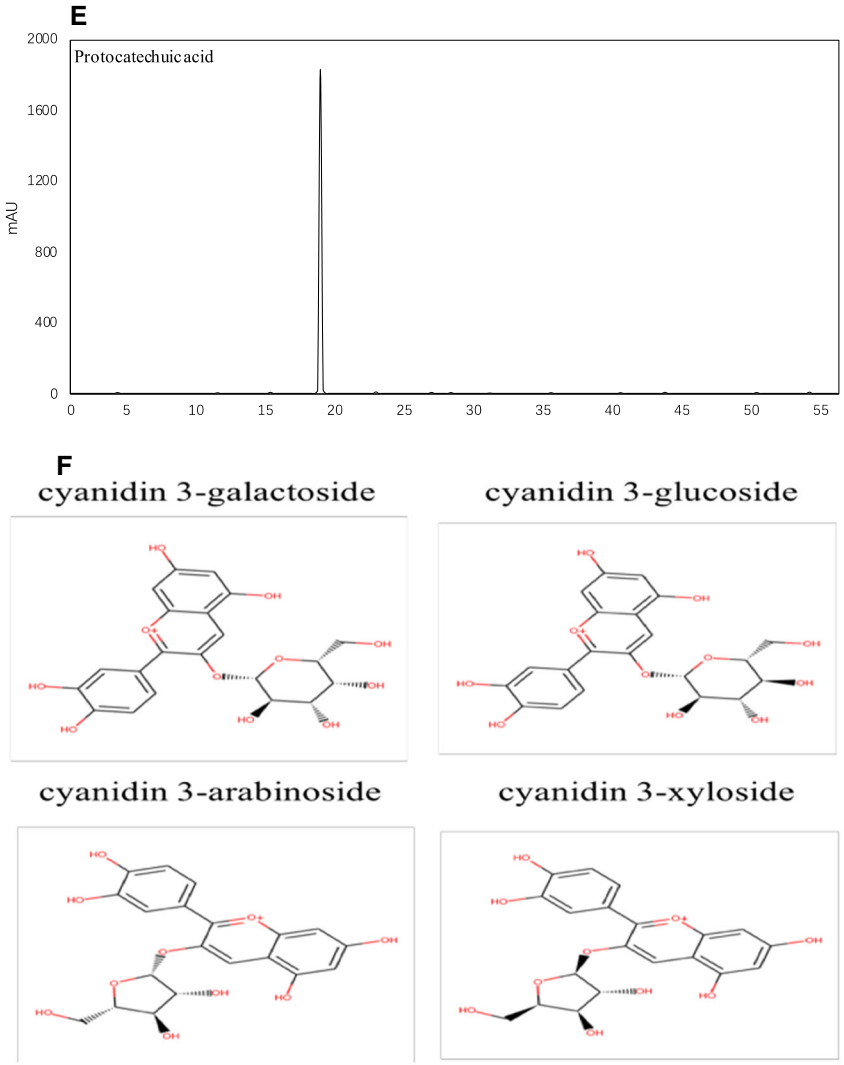

Table 1 Results of HPLC–MS analysis

Peak	Time	MS	MS/MS	Anthocyanin identification
1	24.87	449	287	Cyanidin-3-galactoside
2	25.71	449	287	Cyanidin-3-glucoside
3	26.88	419	287	Cyanidin-3-arabinoside
4	29.18	419	287	Cyanidin-3-xylose

of anthocyanin. The glycosidic bonds of anthocyanins are hydrolyzed by microbial communities, and glycosidic ligands produce phenolic acids and other metabolites. Regulation of AMA by intestinal microorganisms is an important factor in the bioavailability of anthocyanins. The intestinal flora in the colon can secrete a variety of metabolic enzymes, such as β-glucosidase, β-glucoaldolase, which can catalyze the deglycosylation of glycosidic

Table 2 Contents of anthocyanin in samples under different digestion and fermentation times (mg/g)

Anthocyanins contents (mg/g)				
	Undigested	Gastric digestion	Intestinal digestion	Fecal fermentation
Cyanidin-3-galactoside	5.74 ± 0.14	4.12 ± 0.97	1.71 ± 0.74	0.65 ± 0.51
Cyanidin-3-glucoside	0.31 ± 0.03	0.22 ± 0.85	0.09 ± 0.25	/
Cyanidin-3-arabinoside	2.09 ± 0.27	1.54 ± 1.21	0.57 ± 0.17	0.19 ± 0.46
Cyanidin-3-xylose	0.43 ± 0.02	0.31 ± 0.56	0.11 ± 0.34	/
Protocatechuic acid	/	/	/	0.31 ± 0.53

polyphenols and the hydrolysis of esterified phenolic acids (Huang et al. 2018). Among the known common fruits, the antioxidant activity of Black Chokeberry is the highest (Zhang et al. 2018). The results showed that there was a short-term increase in plasma antioxidant capacity after ingestion of cyanidin rich blood orange juice, which may be related to a large increase in protocatechuic acid, a degradation product of cyanidin in a short period of time. Four anthocyanin monomers showed different degrees of decrease in AMA after simulated gastric digestion (Fig. 2b), and further increase in the loss rate after simulated intestinal digestion (Fig. 2c). Digestive enzymes in the digestive process of stomach and small intestine will cause the loss of most anthocyanins, the greater the loss rate, the worse the stability. The more anthocyanins on methoxy substituted anthocyanin glycosyl ligands, the more stable the anthocyanins are. On the contrary, the more hydroxyl groups on glycosyl ligands, the more unstable they are (Dai et al. 2009). The results of the experiment accord with the general law of anthocyanin stability. After colon fermentation (Fig. 2d), the four components of anthocyanins were reduced to anthocyanin-3-galactoside and anthocyanin-3-arabinoside respectively.

Effects of simulated in vitro reactions on DPPH inhibition rate and T-AOC values

The determination of DPPH inhibition rate and T-AOC value is a common method to evaluate the antioxidant capacity of plant tissues. The changes of antioxidant capacity of the samples before and after digestion were measured by simulating the changes of DPPH inhibition rate and T-AOC value in vitro. It can be seen from Fig. 3a that the clearance rate of undigested DPPH in black fruit gland extract is 72.2%. The clearance rate of DPPH was 63.4% and 57.1% after 1 and 2 h in the stomach. The clearance rate of DPPH decreased to 36.45% and 32.75% after 1 and 2 h of enteral digestion, respectively. As can be seen from Fig. 3b, compared with the undigested sample, the digestion of the stomach showed a slight downward trend at 1H ($P > 0.5$), and the T-AOC value decreased significantly with the progress of digestion ($P < 0.05$). After digestion for 2 h, T-AOC reduced to 62.89u/mg, and 26.71% in undigested. The results showed that the T-AOC value of AMA was significantly reduced by in vitro digestion.

Effect of AMA on intestinal microbiota

As can be seen from Fig. 4a, at the level of gate, the intestinal flora is mainly composed of *Actinobacteria*, *Bacteroides*, *Proteobacteria* and *Firmicutes*. AMA significantly increased the proportion of *Bacteroides* (Fig. 4b), which was associated with weight loss. *Bacteroides*, as a beneficial intestinal flora, can help the host decompose polysaccharides and improve nutritional utilization (Yoon et al. 2017). Accelerate the formation of intestinal mucosal vessels and the development of the immune system to enhance the host's immunity (Rosacmillán et al. 2020). *Bacteroides* V1-5482 (atcc29148, isolated from the feces of healthy people), which is usually found in the human small intestine at the end of the small intestine, is considered as a model strain affecting gene expression in the intestine by researchers (Liang et al. 2016). Its gene leader is 6.26 MB. Among the 4779 proteins encoded by the genome, the most important are enzymes involved in the degradation and absorption of polysaccharides, carbohydrates on the cell surface, proteins involved in the synthesis of capsular polysaccharides (such as glycosyltransferase), environmental sensing and signals. Transducing proteins (single or double protein system, type sigma factor) and some proteins related to DNA translocation, which not only have effect on *Bacteroides* themselves, but also have complementary effect on host function (Weller et al. 2000). AMA reduced the proportion of *Firmicutes* (Fig. 4c). And studies showed that *Bacteroides* were positively correlated with obesity. It is a useful biomarker of obesity (Yang et al. 2016). AMA increased the abundance of *Actinobacteria* (Fig. 4), and studies showed that *Actinobacteria* had more antitumor activity (Yabe et al. 2017). Bioactive substances produced by AMA have *Actinobacteria* characteristics and a high proportion of enzyme activity (Sangkanu et al. 2017). AMA showed similar effects as reported in the literature, indicating that AMA has potential weight loss, anticancer and antibacterial effects.

At the genus level, the intestinal flora is mainly composed of *Bifidobacteria, Blautia*, *Klebsiella*, *Escherichia/Shigella*, *Enterococcus*, *Lactobacillus*, *Clostridium*, *Streptococcus*, *Prevotella*, *Clostridium*, *Fecal bacillus* and *Macromonas* (Fig. 5a). Compared with the control group, AMA increased the abundance of *Bifidobacteria* (Fig. 5b), which is the dominant bacteria in the normal intestinal flora of infants (Wang et al. 2018). *Bifidobacteria* can produce organic acids in the gut, reduce the pH based redox potential in the gut, inhibit the invasion of pathogenic bacteria and pathogens, maintain the intestinal microecological balance, and thus produce spatial protection (Azm et al. 2018). The extracellular glycosidase produced by *Bifidobacterium* can degrade the complex polysaccharide of intestinal epithelial cells as potential pathogenic bacteria and endotoxin binding receptor, so as to reduce the adhesion of potential pathogenic bacteria and their toxins to intestinal epithelial cells (Young Oh et al. 2018). AMA promotes the growth of *Blautia* (Fig. 5c), and studies show that *Blautia* helps to clear the gas in the intestine and is related to the change of host phenotype (Burapan et al.

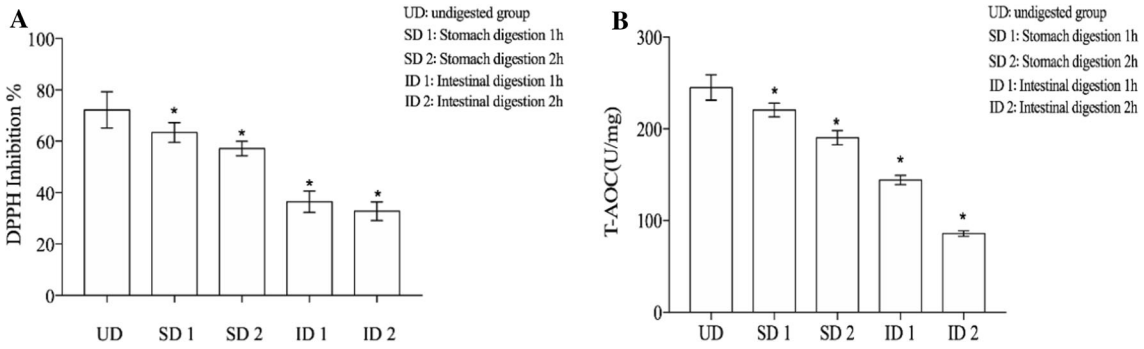

Fig. 3 Effect of UD group, SD 1 group, SD 2 group, ID 1 group, ID 2 group on DPPH inhibition and T-AOC Values are means of three experiments performed in triplicate (three independent measures), with standard deviations depicted by vertical bars. **a** DPPH inhibition, **b** T-AOC Values. Mean values were significantly different from those of the control group: $*p < 0.05$

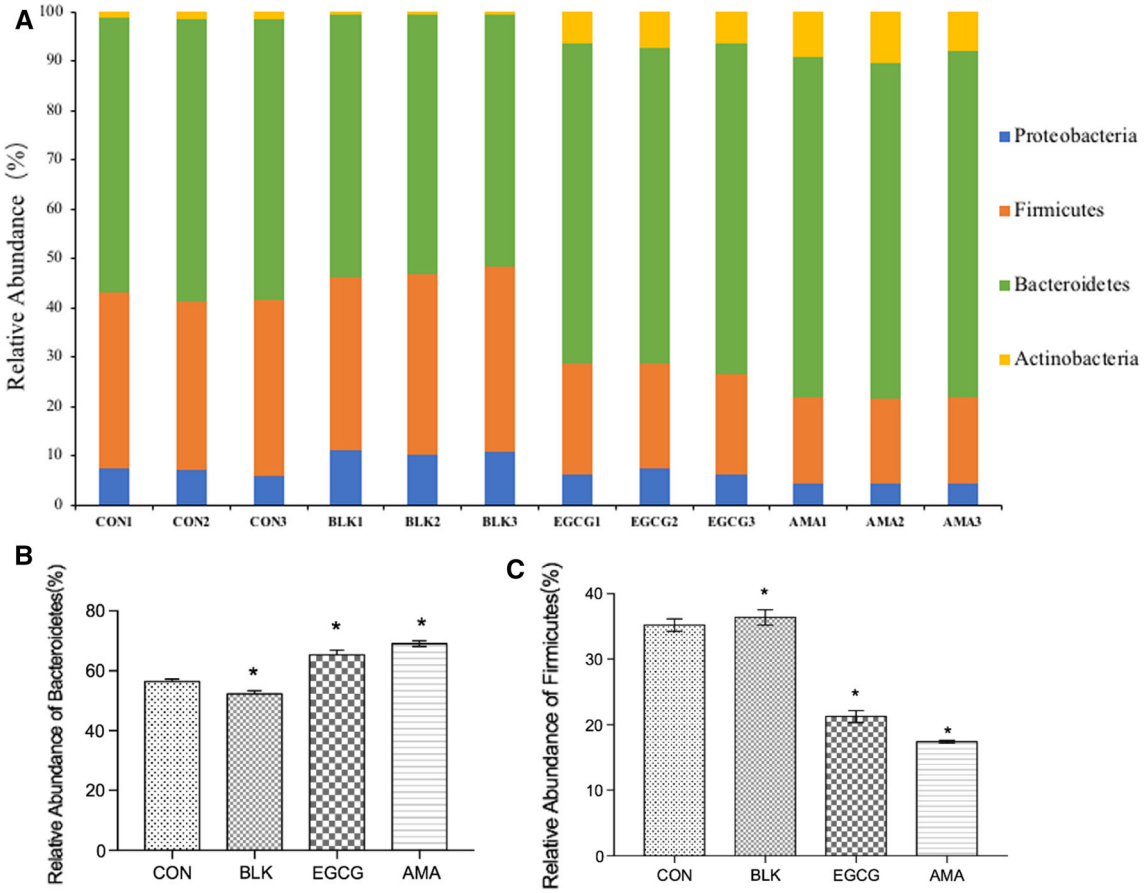

Fig. 4 Microbial compositions of CON group, BLK group, EGCG group and AMA at phylum level. **a** Column diagram of microbial composition; **b** Relative abundance Bacteroidetes; **c** Relative abundance of Firmicutes. Values are means of three experiments performed in triplicate (three independent measures), with standard deviations depicted by vertical bars. Mean values were significantly different from those of the control group: $*p < 0.05$

2017). AMA reduces the abundance of *Prevotella*, *Macromonas*, *Escherichia/Shigella*, *Fusobacteria*, *Klebsiella*, *Enterococcus* and *Streptococcus* (Fig. 5f). The change of the relative abundance of the microbiota caused by AMA may be caused by the anthocyanin metabolites produced by the intestinal microbiota. *Prevotella* thrives in an inflammatory environment, even increasing its own inflammatory advantage (Fig. 5d). 16S rRNA sequencing was used to analyze the excretory microorganisms in untreated patients with new rheumatoid arthritis (NORA), who had too many *Prevotella*. *Prevotella* encodes superoxide reductase and adenosine phosphate sulfonate

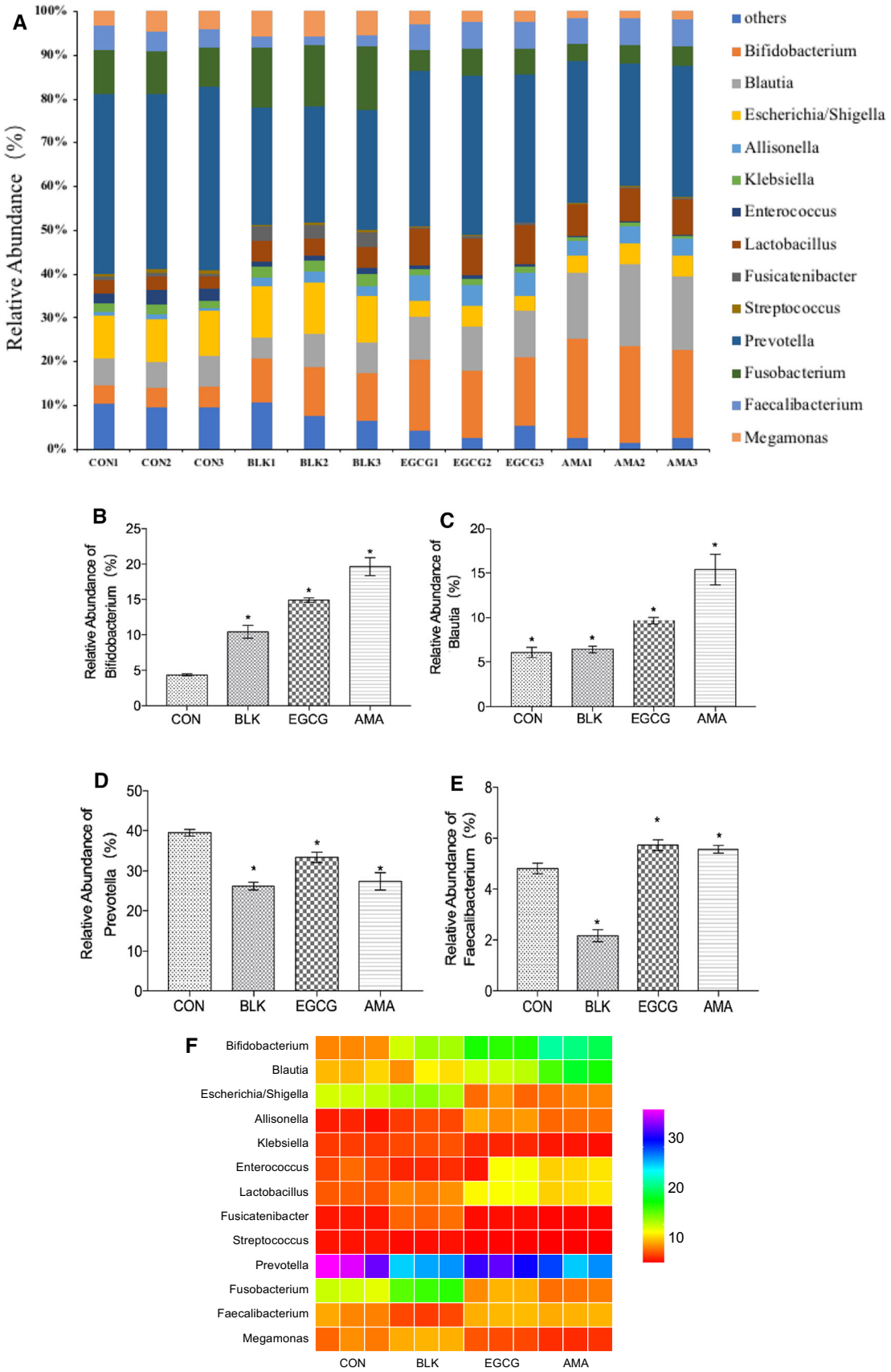
A
Relative Abundance (%)
100%
90%
80%
70%
60%
50%
40%
30%
20%
10%
0%
CON1
CON2
CON3
BLK1
BLK2
BLK3
EGCG1
EGCG2
EGCG3
AMA1
AMA2
AMA3
others
Bifidobacterium
Blautia
Escherichia/Shigella
Allisonella
Klebsiella
Enterococcus
Lactobacillus
Fusicatenibacter
Streptococcus
Prevotella
Fusobacterium
Faecalibacterium
Megamonas
B
Relative Abundance of Bifidobacterium (%)
C
Relative Abundance of Blautia (%)
D
Relative Abundance of Prevotella (%)
E
Relative Abundance of Faecalibacterium (%)
CON
BLK
EGCG
AMA
F
Bifidobacterium
Blautia
Escherichia/Shigella
Allisonella
Klebsiella
Enterococcus
Lactobacillus
Fusicatenibacter
Streptococcus
Prevotella
Fusobacterium
Faecalibacterium
Megamonas
30
20
10

◀**Fig. 5** Microbial compositions of CON group, BLK group, EGCG group and AMA at genus level. **a**, Column diagram of microbial composition at genus level; **b** Relative abundance Bifidobacterium; **c** Relative abundance of Blautia; **d** Relative abundance of Prevotella; **e** Relative abundance of Faecalibacterium; **f** Heatmap at genus level. Values are means of three experiments performed in triplicate (three independent measures), with standard deviations depicted by vertical bars. Mean values were significantly different from those of the control group: $*p < 0.05$.

reductase. These two genes may promote the development and maintenance of intestinal inflammation by increasing *Prevotella's* resistance to active oxygen species from the host and by producing redox protein thioredoxin (Park et al. 2019). AMA increased the number of fecal bacteria (Fig. 5e), and the microecological imbalance caused by fecal bacteria changes was closely related to the incidence of some intestinal diseases. Studies have shown that fecal bacteria can provide energy for the intestinal tract of the production of butyrate, and play an anti-inflammatory role, thus significantly improved intestinal inflammation (Lonneke et al. 2015). Cardona demonstrated that *Lactobacilli*, *Bifidobacteria*, *Bacillus* and *Eubacteria* are involved in the biotransformation of intestinal anthocyanins (Moroz 2002), AMA increased the abundance of *Lactobacillus*, which regulated the balance of intestinal flora, enhanced immunity and resistance, and promoted the growth and development of intestinal tract (Finotti et al. 2009). Therefore, AMA can not only improve the structure of intestinal microflora by regulating the growth of beneficial microorganisms, but also proliferate the microflora related to anthocyanin metabolism.

Conclusion

The experimental results show that the simulated before and after vitro gastrointestinal digestion and colonic fermentation can significantly reduce the total polyphenols and total anthocyanins content in the extract from Black Chokeberry (*Aronia melanocarpa* (Michx.) Elliot) extracts; By measuring the DPPH inhibition rate and T-AOC value of samples before and after gastrointestinal digestion, it was found that in vitro gastrointestinal digestion can significantly reduce the antioxidant capacity of the extract from Black Chokeberry (*Aronia melanocarpa* (Michx.) Elliot). AMA can increase the abundance of beneficial bacteria such as *Bifidobacterium,* reduce the abundance of harmful bacteria and cause changes in intestinal microecology. In order to determine the actual impact on consumption of anthocyanins on human health, further study on the digestion of anthocyanins in vivo is needed.

Acknowledgements This research was supported by "Liaoning Talent Program" Project in Liaoning Province (XLYC1902081).

Compliance with ethical standards

Conflict of interest The authors declare no conflict of interests.

Ethical approval This experiment strictly abides by the ethical principles of human experiments, and the experimental methods and purposes conform to the ethical standards and international practices of human beings.

References

Alara OR, Abdurahman NH, Mudalip SKA, Olalere OA (2017) Characterization and effect of extraction solvents on the yield and total phenolic content from *Vernonia amygdalina* leaves. J Food Meas Charact 12:311–316

Appel K, Meiser P, Millan E, Collado JA, Rose T, Gras CC (2015) Chokeberry (*Aronia melanocarpa* (Michx.) Elliot) concentrate inhibits NF-kappa B and synergizes with selenium to inhibit the release of pro-inflammatory mediators in macrophages. Fitoterapia 105:73–82

Azm SAN, Djazayeri A, Safa M, Azami K, Ahmadvand B, Sabbaghziarani F (2018) Lactobacilli and bifidobacteria ameliorate memory and learning deficits and oxidative stress in β-amyloid (1–42) injected rats. Appl Physiol Nutr Metab 43:718–726

Burapan S, Kim M, Han J (2017) Demethylation of polymethoxyflavones by human gut bacterium, *Blautia* sp. MRG-PMF1. J Agr Food Chem 65:1620–1629

Bursać Kovačević D, Barba FJ, Granato D, Galanakis CM, Herceg Z, Dragović-Uzelac V (2018) Pressurized hot water extraction (PHWE) for the green recovery of bioactive compounds and steviol glycosides from *Stevia rebaudiana* Bertoni leaves. Food Chem 254:150–157

Chen J, Chen Q, Xie C, Ahmad W, Zhao L (2019) Effects of simulated gastric and intestinal digestion on chitooligosaccharides in two in vitro models. Int J Food Sci Technol 1:1–10

Chena G, Xiea M, Peng W, Dan C, Hong Y (2017) Digestion under saliva, simulated gastric and small intestinal conditions and fermentation in vitro by human intestinal microbiota of polysaccharides from *Fuzhuan brick* tea. Food Chem 244:331–339

Colin D (2006) Aspects of anthocyanin absorption, metabolism and pharmacokinetics in humans. Nutr Res Rev 19:137–146

Correa J, Allen E, Mcdonald J, Schroeter K, Corredig M, Paliyath G (2014) Stability and biological activity of wild blueberry (*Vaccinium angustifolium*) polyphenols during simulated in vitro gastrointestinal digestion. Food Chem 165:522–531

Dai J, Gupte A, Gates L, Mumper RJ (2009) A comprehensive study of anthocyanin-containing extracts from selected blackberry cultivars: extraction methods, stability, anticancer properties and mechanisms. Food Chem Toxicol 47:837–847

Daniel AO, Lovie M, Malak AH, Reza T (2018) Application of protein-based edible coatings for fat uptake reduction in deep-fat fried foods with an emphasis on muscle food proteins. Trends Food Sci Technol 80:167–174

Fazenda PP, Fonseca M, Carlier J, Leitão J (2019) Identification and validation of microsatellite markers in strawberry tree (*Arbutus unedo* L.). Turk J Agric For 43:430–436

Finotti A, Treves S, Zorzato F, Gambari R, Feriotto G (2009) Upstream stimulatory factors are involved in the P1 promoter

directed transcription of the A β H-J-J locus. BMC Mol Biol 9:110–119
Galanakis MC (2015) Separation of functional macromolecules and micromolecules: from ultrafiltration to the border of nanofiltration. Trends Food Sci Technol 42:44–63
Galanakis CM (2018) Phenols recovered from olive mill wastewater as additives in meat products. Trends Food Sci Technol 79:98–105
Galanakis CM, Tsatalas P, Galanakis IM (2018) Implementation of phenols recovered from olive mill wastewater as UV booster in cosmetics. Ind Crop Prod 111:30–37
Halasz JA (2010) S-genotyping supports the genetic relationships between Turkish and Hungarian apricot germplasm. J Am Soc Hortic Sci 135:410–417
Gill SR, Pop M, Deboy RT, Eckburg PB, Turnbaugh PJ, Samuel BS (2006) Metagenomic analysis of the human distal gut microbiome. Science 312:1355–1359
Huang Z, Hua Y, Tian Y, Qin C, Gu M (2018) High expression of fructose-bisphosphate aldolase A induces progression of renal cell carcinoma. Oncol Rep 39:2996–3006
Jamar G, Estadella D, Pisani LP (2017) Contribution of anthocyanin-rich foods in obesity control through gut microbiota interactions. BioFactors 43:507–516
Ji B (2014) Stability and absorption of anthocyanins from blueberries subjected to a simulated digestion process. Int J Food Sci Nutr 65:440–448
Jung H, Lee HJ, Cho H, Lee K, Kwak HK, Hwang KT (2015) Anthocyanins in Rubusfruits and antioxidant and anti-inflammatory activities in RAW 264.7 cells. Food Sci Biotechnol 24:1879–1886
Kulling S, Rawel H (2008) Chokeberry (*Aronia melanocarpa*)—a review on the characteristic components and potential health effects. Planta Med 74:1625–1634
Lee KM, Min K, Choi O, Kim KY, Woo HM, Kim Y (2015) Electrochemical detoxification of phenolic compounds in lignocellulosic hydrolysate for *Clostridium* fermentation. Bioresour Technol 187:228–234
Liang G, Malmuthuge N, Bao H, Stothard P, Griebel PJ, Guan LL (2016) Transcriptome analysis reveals regional and temporal differences in mucosal immune system development in the small intestine of neonatal calves. BMC Genom 17:602–611
Lonneke O, Richard D, Karolien VD, Celine DM, Karen V, Freddy H (2015) Steering endogenous butyrate production in the intestinal tract of broilers as a tool to improve gut health. Fron Vet Sci 2:75–76
Moroz VM (2002) Roles of the caudate nuclei, cerebellum, and caudato-cerebellar interconnections in the control and coordination of ballistic food-procuring movements. Neurophysiol 34:395–405
Nagarajan J, Krishnamurthy NP, Nagasundara Ramanan R, Raghunandan ME, Galanakis CM, Ooi CW (2019) A facile water-induced complexation of lycopene and pectin from pink guava byproduct: extraction, characterization and kinetic studies. Food Chem 296:47–55
Nilufer-Erdil D (2014) Investigating the effects of food matrix and food components on bioaccessibility of pomegranate (*Punica granatum*) phenolics and anthocyanins using an in-vitro gastrointestinal digestion model. Food Res Int 62:1069–1079
Oh SY, Youn SY, Park MS, Baek NI, Ji GE (2018) Synthesis of stachyobifiose using bifidobacterial α-galactosidase purified from recombinant *Escherichia coli*. J Agric Food Chem 66:1184–1190
Park GS, Min HP, Shin W, Zhao C, Kim HJ (2017) Emulating host-microbiome ecosystem of human gastrointestinal tract in vitro. Stem Cell Rev 13:1–14
Park SN, Lim YK, Shin JH, Jo E, Kook JK (2019) *Prevotella koreensis* sp. nov., isolated from human subgingival dental plaque of periodontitis lesion. Curr Microbiol 76:1055–1060
Puupponen-Pimia R, Nohynek L, Hartmann SS, Heinonen M, Oksman KM (2005) Berry phenolics selectively inhibit the growth of intestinal pathogens. J Appl Microbiol 98:991–1000
Rivière J (1997) Differentiation between naproxen, naproxen-protein conjugates, and naproxen-lysine in plasma via micellar electrokinetic capillary chromatography—a new approach in the bioanalysis of drug targeting preparations. Clin chem 43:2083
Rosacmillán J, OronaPadilla JL, Florescmoreno VM, SernaSaldivar SO (2020) Effect of Jet-cooking and hydrolyses with amylases on the physicochemical and in vitro digestion performance of whole chickpea flours. Pediatr Res 32:145–148
Ryu D, Koh E (2018) Stability of anthocyanins in bokbunja (*Rubus occidentalis* L.) under in vitro gastrointestinal digestion. Food Chem 30:157–162
Şahin S, Elhussein E, Bilgin M, Lorenzo JM, Barba FJ, Roohinejad S (2018) Effect of drying method on oleuropein, total phenolic content, flavonoid content, and antioxidant activity of olive (*Olea europaea*) leaf. J Food Process Preserv 42:e13604
Sangkanu S, Rukachaisirikul V, Suriyachadkun C, Phongpaichit S (2017) Evaluation of antibacterial potential of mangrove sediment-derived actinomycetes. Microb Pathog 112:303–312
Senica MS, Mikulic PM (2019) Different extraction processes affect the metabolites in blue honeysuckle (*Lonicera caerulea* L. subsp. edulis) food products. Turk J Agric For 43:576–585
Sun D, Huang S, Cai S, Cao J, Han P (2015) Digestion property and synergistic effect on biological activity of purple rice (*Oryza sativa* L.) anthocyanins subjected to a simulated gastrointestinal digestion in vitro. Food Res Int 78:114–123
Suzihaque MUH, Ibrahim UK, Hashib SA, Asri NASM (2017) Antioxidant determination of fiber-enriched milk powder. Adv Sci Lett 23:3897–3902
Swer TL, Mukhim C, Bashir K, Chauhan K (2018) Optimization of enzyme aided extraction of anthocyanins from *Prunus nepalensis* L. LWT Food Sci Technol 91:382–390
Tanaka A (2001) Chemical components and characteristics of black chokeberry. Nip Sho Kogyo Gak 48:606–610
Turroni F, Milani C, Duranti S, Ferrario C, Ventura M (2017) Bifidobacteria and the infant gut: an example of co-evolution and natural selection. Cell Mol Life Sci 75:1–16
Wang M-L, Shen X, Ge L, He M, He F (2018) A preliminary study of the difference in composition of intestinal bifidobacteria between healthy infants and infants with allergic diseases. Chin J Contemp Pediatr 20:746–752
Wang Y, Zhao F, Zhang H, Fk D, Gao QT, Yu Y (2019) Contribution of digestive enzymes in simulated digestion of small intestine to digestibility of gross energy and crude protein of feed for pigs. Chin J Anim Nutr 37:3242–3250
Weller R, Glöckner FO, Amann R (2000) 16S rRNA-targeted oligonucleotide probes for the in situ detection of members of the phylum *Cytophaga-Flavobacterium-Bacteroides*. Syst Appl Microbiol 23:107–114
Worsztynowicz P, Napierala M, Bialas W, Grajek W, Pancreatic OM (2014) Pancreatic α-amylase and lipase inhibitory activity of polyphenolic compounds present in the extract of black chokeberry (*Aronia melanocarpa* L.). Process Biochem 49:1457–1463
Yabe S, Sakai Y, Abe K, Yokota A (2017) Diversity of *Ktedonobacteria* with actinomycetes-like morphology in terrestrial environments. Microbes Environ 32:61–70
Yang JY, Lee YS, Kim Y, Lee SH, Ryu S, Fukuda S (2016) Gut commensal *Bacteroides acidifaciens* prevents obesity and improves insulin sensitivity in mice. Mucosal Immunol 1:104–116

Yoon S, Yu J, Mcdowell A, Kim SH, Ko GP (2017) Bile salt hydrolase-mediated inhibitory effect of *Bacteroides ovatus* on growth of *Clostridium difficile*. J Microbiol 55:892–899

Yuki S, Tadashi S, Koji N, Hirokazu T (2018) Identification of phenol- and p-cresol-producing intestinal bacteria by using media supplemented with tyrosine and its metabolites. FEMS Microbiol Ecol 94:1–11

Zhang S, Zhao J, Xie C, Tan M, Li H (2018) Analysis and development proposals of *Aronia mealnocarpa* planting industry in Heilongjiang province. Asian Agric Res 10:28–30

Zhang L, Fan G, Ammar Khan M, Yan Z, Beta T (2020) Ultrasonic-assisted enzymatic extraction and identification of anthocyanin components from mulberry wine residues. Food Chem 63:214–225

Zinoviadou KG, Galanakis CM, Grimi N, Boussetta N, Mota MJ, Saraiva JA (2015) Fruit juice sonication: implications on food safety and physicochemical and nutritional properties. Food Res Int 77:743–752